JOURNAL OF SOLID STATE CHEMISTRY 48, 154–160 (1983)

Electrical Conductivity and High Resolution Electron Microscopy Studies of WO_{3-x} Crystals with $0 \leq x \leq 0.28$

WUBESHET SAHLE AND MATS NYGREN

Department of Inorganic Chemistry, Arrhenius Laboratory, University of Stockholm, S-106 91 Stockholm, Sweden

Received November 8, 1982

WO_{3-x} crystals with $0 \leq x \leq 0.28$ have been studied by means of HREM and electrical conductivity measurements. Semiconducting behavior with and E_a of the order 0.06 eV was observed for crystals which, according to the HREM study, contained {102} *CS* planes ($x \simeq 0.03$). Plots of conductivity vs $1/T$ for WO_3 and WO_{3-x} containing disordered {102} *CS* planes are also presented. Metallic behavior was found for crystals with ordered {103} *CS* planes ($x \simeq 0.11$), for $W_{12}O_{34}$ ($x = 0.167$), and for $W_{18}O_{49}$ ($x = 0.28$).

Introduction

Tungsten trioxide undergoes several well-characterized phase transitions at different temperatures. Around room temperature WO_3 has a monoclinic structure (*1, 2*), called *I* in the following, which transforms into a triclinic phase below room temperature (*1, 3–5*). At even lower temperatures, below 230 K, the structure is again monoclinic (*3, 5*); this form is named *II* below. These phase transitions have been shown to be first order (*6–8*).

Reduction of tungsten trioxide to metallic tungsten traverses many intermediary suboxides, WO_{3-x}. The first stage of oxygen loss from WO_3 crystals results in the formation of {102} crystallographic shear (*CS*) planes (*9*). Initially ($0 < x \leq 0.02$), these *CS* planes are distributed at random, i.e., the {102} *CS* planes run in several directions and have greatly varying spacings in regions where they are parallel to each other. For $x \geq 0.02$ the *CS* planes are arranged parallel to each other. Continued reduction leads to the formation of fairly well-ordered arrays of {102} *CS* planes. A complete ordering, implying the formation of Magnéli phases of the W_nO_{3n-1} type, has, however, never been observed.

In the interval $0.07 \leq x \leq 0.13$, {103} *CS* planes are formed, which are quasi-ordered for low x values but become more regularly spaced with increasing degree of reduction. Within this part of the phase diagram, distinct phases of the homologous series of W_nO_{3n-2} are reported (*10–13*). Further reduction results in the formation of two phases with other types of structure: $W_{12}O_{34}$ (*14, 15*) at $x \simeq 0.17$ and $W_{18}O_{49}$ (*16*) at $x = 0.28$, while no ordered phases have been observed in between.

Many investigations have concerned the electrical properties of WO_3 (*4–8, 17–20*). Metallic behavior has thus been observed for the monoclinic *I* phase, while the triclinic one is semiconducting. This transition is associated with a marked change in the conductivity. The monoclinic *II* phase is found to be semiconducting with an acti-

0022-4596/83 $3.00

vation energy of about 0.2 eV. At the triclinic to monoclinic *II* transition temperature, a decrease in conductivity by a factor of 10 is reported.

The available conductivity data for WO_{3-x} refer to a large extent to samples with a very low degree of reduction, typically with $x \leq 0.01$ (*8, 19*). These investigations mainly aim at explaining the mechanism of conduction in WO_3. Metallic behavior has been reported for $W_{18}O_{49}$ (*21*), while $W_{12}O_{34}$ has not been studied with respect to its electrical properties.

This study is an attempt to explore the relationship between stoichiometry, structure, and electrical conductivity in the system WO_{3-x} for $0 \leq x \leq 0.28$. The structure of the crystals used in the conductivity measurements was afterwards studied by means of high resolution transmission electron microscopy, and the composition of the individual crystals was evaluated statistically from the electron micrographs.

Experimental

WO_3 crystals were grown from WO_3 powder (Koch-Light Lab. 99.9%) by chemical transport in an oxygen atmosphere, using water vapor as the transporting agent. The crystals grew in the temperature interval 1073–1173 K, transported from 1323 K with a gradient of 15 K/cm. Yellow, pale green, and light yellowish-brown colored crystals were obtained. The yellow crystals were then reduced by means of a CO/CO_2 gas mixture at about 1270 K, with a double-buffer technique. Details of the preparation methods are given in Refs. (*22*) and (*23*).

The crystals used for the conductivity measurements ranged from 0.15 to 0.02 cm in length. The standard four-probe arrangement was used. The contacts were applied onto the crystals as described elsewhere (*24*). The setup allows recording of resistivities ranging from 10^7 to 10^{-3} Ω. Due to this restriction, conductivity data for WO_3 and $W_{18}O_{49}$ ($x = 0.28$) could only be recorded in the temperature interval 140–400 K. For the other crystals the measurements were extended down to 80 K. The heating and cooling rate was 1% per minute of the current temperature.

Data were recorded from both the heating and cooling parts of a complete cycle, and each crystal was cycled between 400 and 80 K several times, to reveal hysteresis effects. Only for slightly reduced WO_3 crystals were such effects found (see below). Due to the uncertainty in the estimation of the cross section of the irregularly shaped crystals, the error in the absolute value of the conductivity is estimated to be of the order of 25%.

The structure and composition of the crystals used in the conductivity measurements were determined by means of a transmission electron microscope, a Siemens ELMISKOP 102, operated at 125 kV. It was equipped with a double tilt-lift stage and with an image intensifier. The crystals were ground in a silica tube with a silica rod pestle. The fragments so obtained were dispersed in *n*-butanol and collected on perforated carbon films supported by copper grids. Electron diffraction patterns and structure images were recorded from several fragments of each crystal.

A computer-controlled microdensitometer (Joyce-Loebl MDM6) was used for the evaluation of the images. The periodicities along the {102} and {103} *CS* planes (8.5 and 12.0 Å, respectively) were used as internal calibration of the magnification. The average spacings of the *CS* planes were obtained from measurements over a number of *CS* planes, ranging from 10 to 130. The composition of each fragment was then determined from the average *CS* plane spacing, using the formulas W_nO_{3n-1} and W_nO_{3n-2} for fragments exhibiting the {102} and {103} types of *CS*, respectively, as the *n* values are proportional to the spacings (*25, 26*). The composition of a crystal used

in the conductivity measurements was then evaluated as the unweighted mean of the compositions of the fragments.

To see how representative the measured crystals were of the samples from which they were picked, HREM studies were also made of specimens containing fragments originating from many crystals from the same batch. The results of these studies, which have been reported previously (*22*), are given in Table I as gross compositions.

Results

Preparative, structural, and composition data of reduced tungsten oxides are given in Table I. Representative conductivity data are presented in Fig. 1.

The activation energy E_a for conduction has been calculated from the linear part of the log δ vs $1/T$ curve according to the formula $\delta = \delta_0 \exp(-E_a/kT)$. The data presented below refer to the crystals which were examined in the electron microscope after the conductivity measurement. Conductivity measurements were, however, carried out for three or more crystals from each batch. The conductivity curves for these crystals were generally very similar.

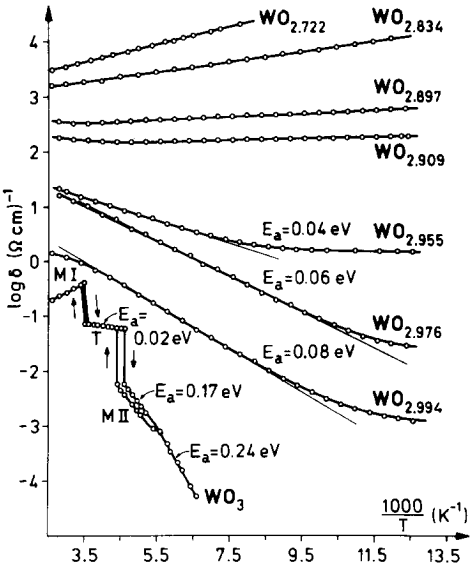

FIG. 1. Conductivity vs $1/T$ plots for WO_3 and WO_{3-x} for $0 < x \leq 0.28$. M*I*, T, and M*II* refer to the monoclinic *I*, triclinic, and monoclinic *II* modifications of WO_3 (see text).

WO_3

The conductivity data for WO_3 given in Fig. 1 are representative for the yellow crystals.

The monoclinic *I* room temperature mod-

TABLE I

PREPARATIVE, STRUCTURAL, AND COMPOSITIONAL DATA OF BATCH PREPARATIONS AND CRYSTALS USED FOR CONDUCTIVITY MEASUREMENTS (STANDARD DEVIATIONS IN PARENTHESES)

	Preparation			Sample			Crystal used for measurements		
Sample	$-\log P_{O_2}$ (atm)	T(°K)	t(hr)	Structure type	No. frag.	Calcul. compos.	Structure type	No. frag.	Calcul. compos.
1	8.79	1267	47	{102}*CS*	23	2.993(6)	{102}*CS*	13	2.994(7)
2	10.45	1265	170	{102}*CS*	13	2.980(12)	{102}*CS*	14	2.976(10)
3	11.19	1271	48	{102}*CS*	27	2.963(20)	{102}*CS*	12	2.963(3)
				{103}*CS*	16	2.904(14)	{103}*CS*	3	2.903(14)
						mean 2.941			mean 2.955
4	11.21	1264	48	{102}*CS*	7	2.957(18)	{102}*CS*	2	2.964(3)
				{103}*CS*	4	2.897(11)	{103}*CS*	13	2.901(5)
						mean 2.935			mean 2.909
5	11.96	1269	46	{103}*CS*	48	2.893(6)	{103}*CS*	11	2.897(4)
6	12.54	1269	59	$W_{12}O_{34}$	21	2.833	{103}*CS*	2	2.869
				$W_{18}O_{49}$	13	2.722	$W_{12}O_{34}$	36	2.833
						Mean 2.789			mean 2.834
7	12.78	1269	72	$W_{18}O_{49}$	32	2.722	$W_{18}O_{49}$	9	2.722

ification of WO_3 exhibits metallic behavior and transforms into a semiconducting triclinic modification at 281 K. The conductivity of the triclinic phase is a factor of six lower than that of the monoclinic *I* phase. From the slope of the log δ vs $1/T$ curve an activation energy (E_a) of 0.02 eV was deduced.

The conductivity drops by a factor of 10 at the triclinic to monoclinic *II* phase transition temperature (218 K). The monoclinic *II* phase is semiconducting. The log δ vs $1/T$ curve for this phase exhibits two different slopes, one for $218 > T > 182$ K, with $E_a = 0.17$ eV, and one for $182 \text{ K} > T > 140$ K, with $E_a = 0.24$ eV.

On heating, the monoclinic *II* to triclinic and the triclinic to monoclinic *I* phase transitions take place at higher temperatures than observed upon cooling: at 227 and 286 K, respectively. A hysteresis effect in the conductivity values was recorded in the temperature region $182 < T < 227$ K (see Fig. 1). The conductivity data and transition temperatures given above did not vary over successive temperature cyclings.

The conductivity curves for light yellowish-brown colored crystals differs in several aspects from the ones discussed above. Each crystal behaves differently, but the curves have some common features. The monoclinic *I* to triclinic transition temperature is thus evident from the conductivity maximum around 280 K. For $280 < T < 330$ K a small decrease in conductivity with increasing temperature is recorded, while the conductivity of the triclinic phase is almost temperature independent. The maximum conductivity value at 280 K is 10–15 times larger than the corresponding value for the yellow crystals. The triclinic to monoclinic *II* transformation occurs at 210 K, and this is associated with a decrease in conductivity of the order of 100–150 times. Finally, the low temperature conductivity data of the light yellowish-brown and the yellow crystals are fairly similar.

The features of the conductivity curves for the green crystals resemble those of the yellow crystals. The two conductivity curves thus almost coincide at the upper and lower ends of the temperature range, but in the intermediary region lower conductivity values are recorded during heating than during cooling. The hysteresis is thus more pronounced for these crystals than for the yellow ones. The discontinuity in the conductivity at the monoclinic *I* to triclinic transition temperature is also smaller for the green crystals.

The yellow, pale green, and light yellowish-brown crystals were examined one by one in the electron microscope. Sharp WO_3-diffraction spots were always observed. The lattice images of the yellow and green crystals showed only the WO_3 pattern, while the images of a few fragments of the light yellowish-brown crystals exhibited small areas where {102} *CS* planes had started to form.

$WO_{2.994}$

The X-ray powder diffraction patterns of the batch indicated a WO_3-type lattice of monoclinic symmetry. HREM examination of the fragments mostly showed randomly oriented {102} *CS* planes. A few fragments with only one or two isolated *CS* planes were also found. Some areas with parallel *CS* planes were also seen, but fragments with random distribution of the {102} *CS* planes in all four equivalent directions were statistically predominant.

The log δ vs $1/T$ curve for a crystal picked from this batch is given in Fig. 1. Semiconducting behavior is observed over the entire temperature range studied. A linear relationship between log δ and $1/T$ is observed for $100 \leq T \leq 225$ K, with $E_a = 0.08$ eV. In the low temperature region E_a increases with increasing temperature, while at high temperatures it decreases.

$WO_{2.976}$

The X-ray powder diffraction pattern of this sample showed a WO_3-lattice of orthorhombic symmetry. Although most of the fragments exhibited parallel but nonperiodic {102} *CS* planes, a few fragments with *CS* planes in several directions were also observed. As shown in Table I, the gross composition and the composition of the crystal used in the conductivity measurements are the same within one standard deviation. One can use the standard deviation of the average n value as a measure of the aperiodic *CS* plane distribution. For this crystal, n values ranging from 25 to 150 were found, with a mean of 55. The distribution has a standard deviation of 37.

From Fig. 1 it is seen that semiconducting behavior is observed over the temperature range studied, with $E_a = 0.06$ eV for $T > 110$ K.

$WO_{2.955}$

The crystal was picked from a batch of gross composition $WO_{2.941}$. Out of 25 fragments studied of this crystal, 22 were found by diffraction to contain {102} *CS* planes. The 3 fragments containing {103} *CS* planes, and 12 {102} *CS* fragments, were used in evaluating the composition of the crystal. The difference in composition between the batch and this crystal thus originated from the difference in the relative occurrence of {103} *CS* planes in the batch and the crystal (Table I). This might indicate that the crystals of this batch contain either predominantly {102} or {103} types of *CS* planes. The distribution of *CS* plane spacings for the {102} *CS* fragments in the crystal is obtained as $n = 27.7 \pm 2.5$.

Three crystals suitable for conductivity measurements were selected from the batch with gross composition $WO_{2.941}$. The conductivity of one of the crystals, labeled $WO_{2.955}$, is given in Fig. 1. The temperature dependence of the conductivity of the second crystal is similar to that of the first one, while the curve of the third one resembles that labeled $WO_{2.909}$ in Fig. 1. This was very likely a crystal containing predominantly {103} *CS* planes (see below). Only the first crystal was analyzed in the electron microscope, however. The $WO_{2.955}$ crystal exhibits semiconducting properties, with $E_a = 0.04$ eV for $T > 140$ K, while E_a decreases with decreasing temperature for $T \leq 140$ K.

$WO_{2.909}$

The crystal used in the conductivity measurements exhibited both {102} and {103} *CS* planes. In this case, however, fragments containing {103} *CS* planes dominated. The composition difference between this crystal and those of the batch (see Table I) can be interpreted in a manner similar to the above. The aperiodicity of the shear plane spacing in this case is much narrower ($n = 20 \pm 1$).

The temperature dependence of the conductivity shows (Fig. 1) metallic behavior in the temperature range $80 \leq T \leq 270$ K, while a small increase of the conductivity with increasing temperature is observed for $T > 270$ K. All three crystals measured showed closely similar electrical behavior.

$WO_{2.897}$

This crystal belongs to a sample in which only {103} *CS* structures were observed. The gross compositions of the sample and of the crystal are in reasonable agreement (Table I). The distribution of *CS* plane spacings is also generally narrow: $n = 19.3 \pm 0.75$.

The conductivity curve of a crystal of the composition $WO_{2.897}$ is given in Fig. 1. As for the $WO_{2.909}$ crystal, metallic behavior is observed for $T \leq 270$ K while σ increases with increasing temperature for $T > 270$ K. The conductivity values of $WO_{2.897}$ seem to be slightly higher than those of $WO_{2.909}$.

$WO_{2.834}$

The fragments of the crystal studied showed mainly the $W_{12}O_{34}$ structure, with frequent twin disorder. Two fragments containing areas of {103} *CS* planes were also observed, but the conductivity curve recorded should, to a good approximation, be representative for the $W_{12}O_{34}$ phase. The batch was found to contain crystals of $W_{12}O_{34}$ and $W_{18}O_{49}$.

The conductivity curve of this compound exhibits metallic behavior over the entire temperature region studied.

$WO_{2.722}$

This crystal was selected from a sample which, according to the X-ray powder diffraction pattern and electron microscopy observations, was a single phase. The cell parameters are a = 18.322(2) Å, b = 3.782(2) Å, c = 14.034(2) Å, and β = 115.21°(2).

The metallic properties of this compound are confirmed, and $W_{18}O_{49}$ is found to be a better conductor than $W_{12}O_{34}$.

Discussion

Salje and Viswanathan (*4*) and Lefkowitz *et al.* (*8*) have shown that WO_3 crystals formed by sublimation and crystals formed from recrystallized molten WO_3 differ slightly in properties and room temperature structure. Thus crystals obtained from melted WO_3 exhibit higher monoclinic *I* to trilinic and triclinic to monoclinic *II* phase transition temperatures that those formed by sublimation. At room temperature the latter possess a monoclinic structure, while the former are triclinic. Our WO_3 crystals, obtained by a chemical transport reaction, have a monoclinic structure according to the X-ray powder patterns; this is consistent with the various transition temperatures reported above.

Berak and Sienko (*19*) have shown that even a very small decrease in the oxygen content of WO_3 gives rise to an increase in the conductivity. The activation energies for conduction in the triclinic and monoclinic *II* phases are reported to increase and decrease, respectively, with decreasing oxygen content of the samples. As our conductivity values of the yellow colored crystals are slightly lower than those reported by, e.g., Berak and Sienko (*19*), and as our E_a values compare favorably with previously reported ones, we conclude that our crystals are very close to WO_3 in stoichiometry.

In this connection it can be noted that Lefkowitz *et al.* (*8*) have suggested that the anomaly in the conductivity curve around 180 K might indicate the presence of another structural transition.

The crystals of WO_{3-x} with $0 \leq x \leq 0.045$ exhibit semiconducting properties. In this part of the phase diagram the parent WO_3 lattice accommodates the oxygen loss by forming {102} *CS* planes. As mentioned above, these planes are arranged differently for various x values. Thus one observed a smooth transition from randomly oriented *CS* planes to parallel and rather periodic *CS* planes via parallel and aperiodic ones, with increasing x values. A similar gradual increase of the conductivity, and decrease of the activation energy, with increasing degree of reduction can be noted. The shape of the log σ vs $1/T$ also changes with the composition.

Berak and Sienko (*19*) reported conductivity data for a crystal picked from a preparation with the gross composition $WO_{2.9877}$. Assuming the composition of this crystal to be the same as that of the batch, one thus would expect that the conductivity and the shape of the conductivity graph would be something intermediary between our curves for $WO_{2.994}$ and $WO_{2.976}$. However, the data presented by Berak and Sienko agree well with our data for $WO_{2.976}$, both

with respect to the conductivity and to the shape of the curve, while their E_a value is slightly higher (0.10 eV) than our value for $WO_{2.976}$ (0.06 eV). This suggests that their crystal might be slightly more oxygen deficient than their batch preparation.

The conductivity values for $WO_{2.909}$ are lower than those for $WO_{2.897}$, while the shapes of the curves are almost identical. Thus both crystals exhibit metallic conductivity below 270 K, and both contain {103} *CS* planes. Barek and Sienko (*19*) reported one conductivity value for 80 K for a crystal from a preparation of the gross composition $WO_{2.895}$, which is about 10 times higher than ours. However, they also stated that $WO_{2.895}$ exhibits metallic behavior in the low-temperature region, with a conductivity minimum around 270 K.

Viswanathan *et al.* (*21*) have performed two probe conductivity measurements on small needle-shaped crystals of $WO_{2.722}$ ($W_{18}O_{49}$). They also found metallic behavior for $W_{18}O_{49}$. Their conductivity values are, however, substantially lower than ours, most probably due to the measuring technique applied.

Acknowledgments

The authors thank Professor Lars Kihlborg for his valuable advice in connection with this work. The cooperation of Dr. Sven Berglund and Dr. Tom Hörlin is also acknowledged. This work has been financially supported by the Swedish Natural Science Research Council.

References

1. S. Tanisaki, *J. Phys. Soc. Japan* **15,** 573 (1960).
2. B. O. Loopstra and H. M. Rietveld, *Acta Crystallogr.* **B25,** 1420 (1969).
3. R. Diehl, G. Brandt, and E. Salje, *Acta Crystallogr.* **B34,** 1105 (1978).
4. E. Salje and K. Viswanathan, *Acta Crystallogr.* **A31,** 356 (1975).
5. S. Tanisaki, *J. Phys. Soc. Japan* **15,** 566 (1960).
6. M. Niino, *J. Phys. Soc. Japan* **33,** 272 (1972).
7. T. Hirose, I. Kawana, and M. Niino, *J. Phys. Soc. Japan* **33,** 22 (1972).
8. I. Lefkowitz, M. B. Dowee, and M. A. Shields, *J. Solid State Chem.* **15,** 24 (1975).
9. R. J. D. Tilley, *Mater. Res. Bull.* **5,** 813 (1970).
10. A. Magnéli, *Ark. Kemi* **1,** 513 (1950).
11. M. Sundberg, *J. Solid State Chem.* **35,** 120 (1980).
12. M. Sundberg, *Acta Crystallogr.* **B22,** 2144 (1976).
13. P. Gado and A. Magnéli, *Acta Crystallogr.* **19,** 1514 (1965).
14. R. Pakering and R. J. D. Tilley, *J. Solid State Chem.* **16,** 247 (1976).
15. M. Sundberg, *Chem. Commun. Univ. Stockholm* **5** (1981).
16. A. Magnéli, *Ark. Kemi* **1,** 233 (1950).
17. T. Hirose, *J. Phys. Soc. Jpn.* **49,** 562 (1980).
18. B. L. Crowder and M. J. Sienko, *Inorg. Chem.* **4,** 73 (1965).
19. J. M. Berak and M. J. Sienko, *J. Solid State Chem.* **2,** 109 (1970).
20. S. Sawada and G. C. Danielson, *Phys. Rev.* **113,** 803 (1959).
21. K. Viswanathan, K. Brandt, and E. Salje, *J. Solid State Chem.* **36,** 45 (1981).
22. S. Berglund and W. Sahle, *J. Solid State Chem.* **36,** 66 (1981).
23. S. Berglund, *Chem. Scr.* **18,** 73 (1981).
24. T. Hörlin, T. Niklewski, and M. Nygren, *Chem. Scr.* **13,** 201 (1978–79).
25. T. G. Allpress and P. Gado, *Crys. Lattice Defects* **1,** 331 (1970).
26. T. G. Allpress, R. J. D. Tilley, and M. I. Sienko, *J. Solid State Chem.* **3,** 440 (1971).